# Quantum Chemical Calculation of Vibrational Spectra of Large Molecules—Raman and IR Spectra for Buckminsterfullerene

**JOHANNES NEUGEBAUER, MARKUS REIHER, CARSTEN KIND, BERND A. HESS**
*Theoretische Chemie, Universität Erlangen-Nürnberg, Egerlandstraße 3, D-91058 Erlangen, Germany*

*Received 27 November 2001; Accepted 11 February 2002*

**Abstract:** In this work we demonstrate how different modern quantum chemical methods can be efficiently combined and applied for the calculation of the vibrational modes and spectra of large molecules. We are aiming at harmonic force fields, and infrared as well as Raman intensities within the double harmonic approximation, because consideration of higher order terms is only feasible for small molecules. In particular, density functional methods have evolved to a powerful quantum chemical tool for the determination of the electronic structure of molecules in the last decade. Underlying theoretical concepts for the calculation of intensities are reviewed, emphasizing necessary approximations and formal aspects of the introduced quantities, which are often not explicated in detail in elementary treatments of this topic. It is shown how complex quantum chemistry program packages can be interfaced to new programs in order to calculate IR and Raman spectra. The advantages of numerical differentiation of analytical gradients, dipole moments, and static, as well as dynamic polarizabilities, are pointed out. We carefully investigate the influence of the basis set size on polarizabilities and their spatial derivatives. This leads us to the construction of a hybrid basis set, which is equally well suited for the calculation of vibrational frequencies and Raman intensities. The efficiency is demonstrated for the highly symmetric $C_{60}$, for which we present the first all-electron density functional calculation of its Raman spectrum.

 J Comput Chem 23: 895–910, 2002

**Key words:** vibrational spectroscopy; quantum chemistry; infrared intensities; Raman intensities; parallel computation; fullerene

## Introduction

Vibrational spectroscopy is one of the most widely used techniques for the determination of molecular structures, for the identification and characterization of molecules, and for reaction control.[1–5] Infrared (IR) and Raman spectroscopy often give complementary information about molecular vibrations (particularly for systems with a center of symmetry). However, only nonstandard methods like the excitation of vibrations via neutron scattering, which require expensive and extended experimental setups, can be applied in the case of modes with zero intensity in both IR and Raman spectra.

In general, vibrational spectra of large molecules with many degrees of freedom are too complicated to yield information about the vibrational motions in detail. Experience and chemical intuition are necessary in order to assign peaks in spectra to particular modes of vibration. In most cases this is not possible at all.

During the last decade, quantum chemical methods, especially those that are based on density functional theory, have matured to become a reliable and routinely applicable diagnostic tool for the assignment of an experimental spectrum. The quantum chemical approach can yield more information than experiment. In principle, all normal modes of a single molecule (including the modes that are neither IR nor Raman active) and the corresponding eigenvalues, that is, the frequencies, can be obtained in a frequency analysis based on the time-independent Schrödinger equation for the stochastic description of the nuclei within the Born-Oppenheimer approximation. Because we are aiming at large molecules, we

***Correspondence to:*** M. Reiher; e-mail: Markus.Reiher@chemie.uni-erlangen.de

Contract/grant sponsor: SFB 583

Contract/grant sponsor: Fonds der Chemischen Industrie

adopt the harmonic approximation that replaces the potential $\bar{E}_{\mathrm{el}}(\mathbf{R})$ by $\bar{E}_{\mathrm{el}}(\mathbf{R}) \approx \mathbf{R}^{(c)\dagger}\mathbf{F}^{(c)}\mathbf{R}^{(c)}$, where $R_j^{(c)}$ are Cartesian nuclear coordinates and $\mathbf{F}^{(c)}$ is the Cartesian Hessian matrix. Here and in the following we denote the expectation value of a quantity in the *electronic degrees of freedom* by an overbar, for example, $\langle\psi(\mathbf{r};\,\mathbf{R})|H_{\mathrm{el}}|\psi(\mathbf{r};\,\mathbf{R})\rangle = \bar{E}_{\mathrm{el}}(\mathbf{R})$, whereas we reserve the bracket notation $\langle \ldots \rangle$ for expectation values of the nuclear degrees of freedom. Within this approximation the nuclear Schrödinger equation in the basis of mass-weighted normal coordinates $\mathbf{R}^{(q)}$ is given by

$$\left(-\frac{\hbar^2}{2}\nabla^{(q)\dagger}\nabla^{(q)} + \mathbf{R}^{(q)\dagger}\mathbf{F}^{(q)}\mathbf{R}^{(q)}\right)|v^{\mathrm{tot}}\rangle = E_{\mathrm{tot}}|v^{\mathrm{tot}}\rangle \qquad (1)$$

$\mathbf{F}^{(q)}$ is the diagonalized Hessian with elements

$$F_{ij}^{(q)} = \left(\frac{\partial^2\bar{E}_{\mathrm{el}}(\mathbf{R}^{(q)})}{\partial R_i^{(q)}\partial R_j^{(q)}}\right)_{\mathrm{eq}} \qquad (2)$$

Because $\mathbf{F}^{(q)}$ is diagonal, eq. (1) represents a system of $3N$ *decoupled* differential equations, one for each normal mode, that is, for a collective motion along an individual normal coordinate. Each single equation for normal coordinate $R_p^{(q)}$ is of the well-known form of a quantum mechanical harmonic oscillator equation with analytically known eigenfunctions $|v_p\rangle$. The total nuclear wave function $|v^{\mathrm{tot}}\rangle$ is given as a product of all single-mode wave functions $|v_p\rangle$, and the total nuclear energy $E_{\mathrm{tot}}$ is the sum over all single-mode energy eigenvalues $\varepsilon_p$. The single-mode wave functions are denoted by their quantum numbers $v_p$, and $v$ characterizes the whole set $\{v_1,\ v_2,\ \ldots,\ v_{3N}\}$ of quantum numbers. Angular frequencies $\omega_p = 2\pi\nu_p$ are then related to the diagonal elements $F_{pp}^{(q)} = \omega_p^2$, and energy eigenvalues result as $\varepsilon_p = \hbar\omega_p(v_p + 1/2)$.

In this article, we demonstrate how such calculations can be performed efficiently, particularly for large molecules using any available quantum chemical method. We discuss the calculation of a harmonic force field for large molecules and the concomitant calculation of IR and Raman intensities. Point group symmetry and parallel implementation can be exploited in order to reduce the computational effort for this task. If the calculations of frequencies and intensities have been performed, the investigation of additional features, like isotope effects, thermochemical data, or charge decomposition analyses in real space (like Cioslowski's analysis based on atomic polar tensors[6]) is straightforward.

In the next section, we shall review the underlying theoretical basis in order to clearly define the quantities that are to be calculated. We deem it necessary to compile all important information in the present article in order to make the work self-contained because all approximations and assumptions must be clearly identified, and the pertinent constants entering the expressions must be given explicitly. Derivations that can be found in standard textbooks are only briefly recalled. The aim of these sections is to outline the connections between the basic quantum mechanical ideas and the quasi-classical approximations. All formulae relevant for the actual calculation of spectra are derived, and their implementation is discussed. The third section demonstrates how to take advantage of the molecular symmetry in our program environment in order to reduce the computational cost, while the fourth section describes the design of the implementation. Finally, the vibrational spectra of Buckminsterfullerene $C_{60}$ are presented in the fifth section as an example for which the use of the point group symmetry and parallel computation drastically decreases the total computational time.

## Calculation of IR and Raman Intensities

In order to calculate intensities of vibrational excitations and to validate the results in the light of all approximations we briefly recall results from time-dependent perturbation theory, where the dimensions for all quantities are given in order to show explicitly how the SI units are connected to the Hartree atomic units used in all quantum chemistry programs. Because the two systems of dimensions are always a source of confusion, we should like to stress this aspect of the derivation.

### *Transition Rates and IR Intensities*

Calculating the IR intensities for a specific transition requires the determination of the transition rate. Within *first order* time-dependent perturbation theory and assuming a continuous range of frequencies that can cause a transition between the initial state $|v_i\rangle$ and the final state $|v_f\rangle$, the rate for the transition $|v_f\rangle \leftarrow |v_i\rangle$ is given by (cf., ref. 7 or ref. 8)

$$W_{f\leftarrow i} = \frac{1}{\hbar^2}\langle H_{fi}^{(1)}\rangle^2\rho_N(\nu_{fi})\left(\frac{1}{\mathrm{s}}\right), \quad \langle H_{fi}^{(1)}\rangle = \langle v_f^{\mathrm{tot}}|H^{(1)}|v_i^{\mathrm{tot}}\rangle \quad (\mathrm{J}) \qquad (3)$$

where $\rho_N(\nu_{fi})$ is the density of photon states per frequency range (Fermi's Golden Rule). Within the dipole approximation, that is, the neglect of contributions from magnetic dipole moments, electric quadrupole moments, and higher order terms,[8] the perturbation is

$$\begin{aligned}\langle H_{fi}^{(1)}\rangle = -\langle v_f^{\mathrm{tot}}|\bar{\boldsymbol{\mu}}(\mathbf{R}^{(q)})\cdot\boldsymbol{\mathscr{E}}|v_i^{\mathrm{tot}}\rangle &\approx -\langle v_f^{\mathrm{tot}}|\bar{\boldsymbol{\mu}}(\mathbf{R}^{(q)})|v_i^{\mathrm{tot}}\rangle\cdot\boldsymbol{\mathscr{E}}_0 \\ &= -\langle\boldsymbol{\mu}_{fi}\rangle\cdot\boldsymbol{\mathscr{E}}_0 \quad (\mathrm{J}) \qquad (4)\end{aligned}$$

assuming that an average amplitude $\boldsymbol{\mathscr{E}}_0$ of the electric field vector $\boldsymbol{\mathscr{E}}$ is essentially constant over the extent of the molecule. The transition dipole matrix element, $\langle\boldsymbol{\mu}_{fi}\rangle = \langle v_f^{\mathrm{tot}}|\bar{\boldsymbol{\mu}}(\mathbf{R}^{(q)})|v_i^{\mathrm{tot}}\rangle$, requires integration over normal coordinates $\mathbf{R}^{(q)}$ of the molecule. Because translational and rotational contributions are still includ-

ed* in $|v^{\text{tot}}\rangle$, it might be useful to write the total nuclear wave function as follows:

$$|v^{\text{tot}}\rangle = |v\rangle \cdot \chi^{\text{rot}} \cdot \chi^{\text{trans}} \tag{5}$$

where $|v\rangle$ is a product of the $(3N - 6)$ [or $(3N - 5)$ for linear molecules, respectively] vibrational single mode wave functions. Omitting rotational and translational contributions, the expression in eq. (4) yields $\langle H_{fi}^{(1)}\rangle^2 = \langle \boldsymbol{\mu}_{fi}\rangle^2 \mathscr{E}_0^2$ if both the electronic dipole moment, $\bar{\boldsymbol{\mu}}(\mathbf{R}^{(q)})$, and $\mathscr{E}_0$ have the same direction. Because molecules are randomly oriented in fluids, a summation over all allowed rotational states would be necessary in order to model the spectrum quantum mechanically. However, almost without loss of accuracy, the classical mean value, $\langle \mu_{fi}^{\text{av}}\rangle^2 = \langle \mu_{fi}\rangle^2/3$, may be applied here instead.

The classical expression for the energy $E_\nu^{\text{EMF}}$ of the electromagnetic field mode with frequency $\nu$ in volume $V$ is $E_\nu^{\text{EMF}} = 2\varepsilon_0 \boldsymbol{\varepsilon}_0^2 V$, such that we may introduce the energy density per frequency range:

$$\rho(\nu) = \frac{E_\nu^{\text{EMF}}}{V}\,\rho_N(\nu) \quad \left(\frac{\text{Js}}{\text{m}^3}\right) \tag{6}$$

The net transition rate for the transition $|v_f\rangle \leftarrow |v_i\rangle$ per unit volume is then given by

$$W_{f\leftarrow i}^{\text{net}} = B_{fi}\rho(\nu_{fi})(N_i - N_f)\left(\frac{1}{\text{s m}^3}\right)$$

$$\text{with} \quad B_{fi} = \frac{1}{6\varepsilon_0\hbar^2}\langle \mu_{fi}\rangle^2 \left(\frac{\text{m}^3}{\text{J s}^2}\right) \tag{7}$$

because the Einstein coefficient for stimulated emission, $B_{if}$, is equal to $B_{fi}$. $N_f$ and $N_i$, respectively, denote the number of molecules per unit volume in the final state.

In the case of IR spectroscopy, the intensity per frequency interval, $I(\nu)$, emitted by a radiation source at frequency $\nu$ is defined as the energy $\Delta E$ that passes through an area $A$ within the time interval $\Delta t$, that is, $I(\nu)d\nu = \Delta E/(A\Delta t)$. Taking into account that the radiation source always shows a finite range of frequencies, we may write the total intensity of the light source in this range as

$$I_\nu := \int_{\text{range}} I(\nu)d\nu = I(\nu)\Delta\nu \quad \left(\frac{\text{J}}{\text{s m}^2}\right) \tag{8}$$

where the intensity per frequency range is assumed to be almost constant in the range $\Delta\nu$ of the line width of the radiation source.

If we consider an element of absorbing material of length $dl$ and cross section $A = V/dl$, every transition $|v_f\rangle \leftarrow |v_i\rangle$ in this element will decrease the energy of the radiation field by an amount of $\Delta E = h\nu_{fi}$, such that the total decrease of intensity is given by[9]

$$-dI_{\nu_{fi}} = h\nu_{fi}W_{f\leftarrow i}^{net}dl = h\nu_{fi}B_{fi}\rho(\nu_{fi})(N_i - N_f)dl \quad \left(\frac{\text{J}}{\text{s m}^2}\right) \tag{9}$$

because $W_{f\leftarrow i}^{net}V$ is the number of transitions in the element of volume $V$ per time interval $\Delta t$. With the relation $\rho(\nu) = I(\nu)/c = I_\nu/(c\Delta\nu)$ (cf. ref. 8) eq. (9) leads to a homogeneous differential equation with the solution

$$I_{\nu_{fi}} = I_{0,\nu_{fi}}\exp[-\kappa(\nu_{fi})Cl] \quad \left(\frac{\text{J}}{\text{s m}^2}\right) \tag{10}$$

where $l$ is the total length of the sample chamber. The absorption coefficient $\kappa(\nu_{if})$ is given as

$$\kappa(\nu_{fi}) = \frac{1}{C}\frac{h\nu_{fi}}{c\Delta\nu}B_{fi}(N_i - N_f) \quad \left(\frac{\text{m}^2}{\text{mol}}\right) \tag{11}$$

where $C$ is the molar concentration of the absorbing material.

Because the absorption lines always have a finite width, for the integral absorption coefficient $\mathscr{A}_\nu$ (assuming that $B_{fi}$ is constant in the frequency range) we get

$$\mathscr{A}_\nu = \int_{\text{line}} \kappa(\nu)d\nu = \kappa(\nu)\Delta\nu$$

$$= \frac{1}{C}\frac{h\nu_{fi}}{c}\frac{\langle \mu_{fi}\rangle^2}{6\varepsilon_0\hbar^2} \times (N_i - N_f) \quad \left(\frac{\text{m}^2}{\text{s mol}}\right) \tag{12}$$

For thermal equilibrium, the occupation numbers for the harmonic oscillator may be obtained from the Boltzmann distribution (with the lowest vibrational level as reference point; see ref. 10 for details). The only remaining quantity in eq. (12) that has to be determined from the electronic wave function is the system-specific quantity $\langle \mu_{fi}\rangle^2$. Because the expectation value of the electronic dipole moment $\bar{\mu}(\mathbf{R}^{(q)})$, which enters $\langle \mu_{fi}\rangle^2$, depends on $\mathbf{R}^{(q)}$, a Taylor series expansion (as depicted in the section "Raman Intensities") is necessary.† Considering anharmonicities in the potential in eq. (1) or higher order terms in the series expansion [eq. (21)] for the dipole moment leads to the occurrence of overtones and combination bands.

Taking into account that within this approximation all fundamental transitions $|v_{p,f}\rangle \leftarrow |v_{p,i}\rangle$ for a given normal mode $p$ occur at the same frequency $\nu_{fi} = \nu_p$, it is necessary to sum over all absorption coefficients for these transitions. After this summation

*See the third section for the elimination of rotational and vibrational modes.

†In the case of small molecules, that is, diatomics and triatomics, it is often possible to determine the electronic dipole moment for a sufficiently large number of points on the potential energy surface. In these cases it is possible to perform a numerical integration without using a truncated Taylor series, or to use a suitable fit of $\bar{\mu}(\mathbf{R}^{(q)})$.

the integral absorption coefficient is independent of temperature.[‡] Utilizing eqs. (12), (29), and (28) yields—after summation—the final result

$$\mathcal{A}_\nu = \frac{1}{4\pi\varepsilon_0}\frac{N_A\pi}{3c}\left(\frac{\partial\bar{\mu}}{\partial R_k^{(q)}}\right)_0^2 \quad \left(\frac{\mathrm{m}^2}{\mathrm{s\ mol}}\right) \tag{13}$$

to be calculated with quantum chemical methods. Another frequently used definition for the absorption coefficient is

$$\mathcal{A}_{\tilde{\nu}} = \mathcal{A}_\nu / c \quad (\mathrm{m/mol}) \tag{14}$$

It should be noted that usually not the intensities for a particular transition, but the absorption coefficients are calculated, because they are independent of the experimental setup, that is, the intensity of the incident light, the molar concentration, and the length of the sample cell.

### *Raman Intensities*

The treatment of Raman intensities is based on Placzek's classical theory of polarizability.[11] In the theory of the Raman effect, the intensity is defined as the ratio of the radiation power $d\Phi$ in a conical beam of solid angle $d\Omega$. Within classical electrodynamics the intensity of an oscillating dipole is given as[3]

$$I(\theta) = \frac{\pi^2 c\,\tilde{\nu}_0^4 \mu_{0,\mathrm{ind}}^2(\nu_0)\sin^2(\theta)}{2\varepsilon_0} \quad \left(\frac{\mathrm{J}}{\mathrm{s\ sr}}\right) \tag{15}$$

where $\theta$ is the angle between the direction of propagation of the incident beam and the direction of observation, $\tilde{\nu}_0$ is the wave number of the incident radiation, and $\mu_{0,\mathrm{ind}}(\nu_0)$ is the amplitude of the induced dipole moment that oscillates with the same frequency $\nu_0 = \tilde{\nu}_0 c$ as the incident radiation. Because the intensity of the radiation source is large in general, quantum effects on the radiation field are negligible.[8] However, for the molecular properties a quantum mechanical treatment is required. This approach is usually called a "partial quantum mechanical treatment" of scattering phenomena.

It is necessary to calculate the time-independent amplitudes of the oscillating dipole moment, which are obtained as matrix elements of the induced dipole moment [cf. eq. (4)]:

$$\langle \mu_{0,fi}^{\mathrm{ind}} \rangle = \langle v_f^{\mathrm{tot}} | \bar{\alpha} \cdot \mathscr{E}_0 | v_i^{\mathrm{tot}} \rangle \approx \langle v_f^{\mathrm{tot}} | \bar{\alpha} | v_i^{\mathrm{tot}} \rangle \mathscr{E}_0 \quad (\mathrm{C\ m}) \tag{16}$$

$\mathscr{E}_0$ is the amplitude of the incident electromagnetic field, and $\bar{\alpha}$ is the polarizability of the molecule. We are taking into account only the linear response of the molecule-radiation interaction, that is, effects concerning first and higher hyperpolarizabilities are not considered. Additionally, it is assumed that the electric field vector $\mathscr{E}_0$ is constant within the whole molecule. This is a good approximation as long as the wavelength of the light is large compared to the dimensions of the molecule.

In contrast to the former treatment, we now have to take into account the rotational contributions to the nuclear wave function $|v^{\mathrm{tot}}\rangle$ defined in eq. (5), which will be characterized by the rotational quantum numbers $J$ and $M_J$. This is necessary because the matrix element in eq. (16) depends on the orientation of molecule and radiation beam. The translational contribution is not considered because it does not affect the matrix element. We may utilize the product ansatz:

$$|v^{\mathrm{tot}}\rangle = |v, J, M_J\rangle = |v\rangle \cdot |J, M_J\rangle \tag{17}$$

with $|v\rangle$ defined in eq. (5). This ansatz is only valid if $\nu_0 \gg \nu_{\mathrm{rot}}, \nu_{\mathrm{vib}}$ and $\nu_0 \ll \nu_{\mathrm{elec}}$, where $\nu_{\mathrm{rot}}$, $\nu_{\mathrm{vib}}$, $\nu_{\mathrm{elec}}$ are the frequencies for rotational, vibrational, and electronic transitions of the molecule, and it amounts to the neglect of coupling matrix elements between vibrational and rotational motion. Another requirement for this treatment is that the electronic ground state of the system is nondegenerate.

Because $\bar{\alpha}$ is a tensor, we are concerned with matrix elements of the tensor components:

$$\langle \alpha_{pq,fi} \rangle = \langle v_f | \langle J_f, M_{J,f} | \bar{\alpha}_{pq} | J_f, J_{z,i} \rangle | v_i \rangle \quad \left(\frac{\mathrm{C\ m}^2}{\mathrm{V}}\right), \quad p, q = \{x, y, z\} \tag{18}$$

where the integration over the electronic coordinates has already been carried out, such that $\bar{\alpha}_{pq}$ is the electronic expectation value for a given set of nuclear coordinates. The components of the polarizability tensor depend on the choice of the space-fixed coordinate system. They are related to the components in the molecule-fixed axes $p'$, $q'$ by[§]

$$\bar{\alpha}_{pq} = \sum_{p'q'} \bar{\alpha}_{p'q'} \cos(pp') \cos(qq') \tag{19}$$

The components of the polarizability in the molecular coordinate system do not change under molecular rotation, in contrast to the ones in the space-fixed system. It follows that separation of the integrations over vibrational and rotational coordinates is possible:

$$\langle \alpha_{pq,fi} \rangle = \sum_{p'q'} \langle \alpha_{p'q',fi} \rangle \langle J_f, M_{J,f} | \cos(xx') \cos(yy') | J_i, M_{J,i} \rangle \tag{20}$$

where the matrix element $\langle \alpha_{p'q',fi} \rangle = \langle v_f | \bar{\alpha}_{p'q'} | v_i \rangle$ only depends on the vibrational quantum numbers $\{v_i, v_f\}$ and the electronic state of the molecule, as in the case of the transition dipole moment in eq. (12).

Because $\bar{\alpha}_{p'q'}$ is not known as an explicit function of $\mathbf{R}^{(q)}$ either, but evaluation of the matrix elements $\langle \alpha_{pq,fi} \rangle$ requires integration over nuclear coordinates, a Taylor series expansion is necessary.[‖] The evaluation of the matrix elements for the

[‡]The summation is also necessary for the Raman intensities. See ref. 3 for details.

[§]For a more general treatment see ref. 12.

[‖]Footnote [†] also holds for the polarizability.

components of the polarizability tensor can be performed in exactly the same way as for the components of the dipole moment, which is therefore shown in the following for both cases. In eqs. (25) to (27) we made use of the properties of the Hermite polynomials ($\bar{\mu}$ and $\bar{\alpha}$ are electronic matrix elements).

*Taylor series expansion of electronic matrix elements*

IR

$$\bar{\mu} = \bar{\mu}^{(0)} + \sum_k \left(\frac{\partial \bar{\mu}}{\partial R_k^{(q)}}\right)_0 R_k^{(q)} + O(R_k^{(q)2}) \tag{21}$$

Raman

$$\bar{\alpha} = \bar{\alpha}^{(0)} + \sum_k \left(\frac{\partial \bar{\alpha}}{\partial R_k^{(q)}}\right)_0 R_k^{(q)} + O(R_k^{(q)2}) \tag{22}$$

*Evaluation of the total matrix elements, including nuclear wave functions [neglecting quadratic and higher order terms from eqs. (21) and (22)]*

$$\langle \mu_{fi} \rangle = \bar{\mu}^{(0)} \langle v_f | v_i \rangle + \sum_k \left(\frac{\partial \bar{\mu}}{\partial R_k^{(q)}}\right)_0 \langle v_f | R_k^{(q)} | v_i \rangle \tag{23}$$

$$\langle \alpha_{fi} \rangle = \bar{\alpha}^{(0)} \langle v_f | v_i \rangle + \sum_k \left(\frac{\partial \bar{\alpha}}{\partial R_k^{(q)}}\right)_0 \langle v_f | R_k^{(q)} | v_i \rangle \tag{24}$$

*Evaluation of matrix elements $\langle v_f | v_i \rangle$ and $\langle v_f | R_k^{(q)} | v_i \rangle$*

$$\langle v_f | v_i \rangle = \prod_{p=1}^{3N-6} \langle v_{p,f} | v_{p,i} \rangle = \prod_{p=1}^{3N-6} \delta_{v_{p,f}, v_{p,i}} \tag{25}$$

$$\langle v_f | R_k^{(q)} | v_i \rangle = \langle v_{k,f} | R_k^{(q)} | v_{k,i} \rangle \cdot \prod_{p=1, p\neq k}^{3N-6} \langle v_{p,f} | v_{p,i} \rangle \tag{26}$$

$$\langle v_{k,f} | R_k^{(q)} | v_{k,i} \rangle = \begin{cases} (v_{k,i}+1)^{1/2} b_{v_k}; & v_{k,f} = v_{k,i} + 1 \\ (v_{k,i})^{1/2} b_{v_k}; & v_{k,f} = v_{k,i} - 1 \\ 0; & \text{otherwise} \end{cases} \tag{27}$$

$$b_{v_k}^2 = \frac{\hbar}{2\omega_k} = \frac{\hbar}{4\pi\nu_k} = \frac{\hbar}{8\pi^2 c \tilde{\nu}_k} \tag{28}$$

*Summary of the above equations for fundamental transitions $|v_{k,i} + 1\rangle \leftarrow |v_{k,i}\rangle$*

$$\langle \mu_{fi} \rangle = b_{v_k} (v_{k,i}+1)^{1/2} \left(\frac{\partial \bar{\mu}}{\partial R_k^{(q)}}\right)_0 \tag{29}$$

$$\langle \alpha_{fi} \rangle = b_{v_k} (v_{k,i}+1)^{1/2} \left(\frac{\partial \bar{\alpha}}{\partial R_k^{(q)}}\right)_0 \tag{30}$$

It should be remembered that $|v^{\text{tot}}\rangle$ is within the harmonic approximation (mechanical harmonicity) a product of the individual harmonic oscillator wave functions for all normal modes of the molecule. Because also the Taylor series for $\bar{\mu}$ and $\bar{\alpha}$ are truncated after the quadratic terms (electrical harmonicity), the procedure presented here is called the double harmonic approximation.

From eq. (27) it follows that nonvanishing contributions for the scattering intensity occur for all transitions with $\delta v_k = 0, \pm 1$. The case $\delta v_k = 0$ corresponds to Rayleigh scattering, that is, the frequency of the incident radiation remains unchanged. For Raman scattering, where we restrict ourselves to the Stokes case with $v_{k,f} = v_{k,i} + 1$, the wave number $\bar{\nu}_0$ of the oscillating induced dipole is no longer $\tilde{\nu}_{\text{in}}$, the wave number of the incident beam, but it has to be replaced by $\tilde{\nu}_{\text{in}} - \tilde{\nu}_p$, where $\tilde{\nu}_p$ is the wave number of the vibrational transition for normal mode $p$.

We will consider the following experimental setup as a typical example:[#] The incident beam is directed along the $z$-axis of the space-fixed Cartesian coordinate system, and is plane-polarized in $y$ direction. The observation is carried out along the $x$-axis ($\theta = \pi/2$) without any analyzers in the scattered beam, that is, the scattered radiation that is plane polarized along the $y$ and $z$ axis will be detected. According to eq. (16), the amplitude of the induced dipole moment is then obtained as

$$\langle \mu_0^{\text{ind}} \rangle^2 = \langle \mu_{0,y}^{\text{ind}} \rangle^2 + \langle \mu_{0,z}^{\text{ind}} \rangle^2 = (\langle \alpha_{yy,fi} \rangle + \langle \alpha_{zy,fi} \rangle) \mathscr{E}_0^2 \quad (\text{C}^2\,\text{m}^2) \tag{31}$$

[#]The implementation presented in the section "Example: Buckminsterfullerene $C_{60}$" can, of course, handle equations for any experimental setup.

because $\mathscr{E}_{0,x} = \mathscr{E}_{0,z} = 0$ and $\mathscr{E}_{0,y} = |\mathscr{E}_0|$. With this expression, we may write eq. (15) as

$$I(\pi/2) = \frac{\pi^2 c(\tilde{\nu}_{\text{in}} - \tilde{\nu}_p)^4}{2\varepsilon_0} \mathscr{E}_0^2(\langle\alpha_{yy,fi}\rangle^2 + \langle\alpha_{zy,fi}\rangle^2) \quad \left(\frac{\text{J}}{\text{s sr}}\right) \quad (32)$$

For a scattering volume containing $N_i$ molecules in the vibrational state $|v_{p,i}\rangle$, a classical averaging over all cosine terms in eq. (19), which replaces the quantum mechanical integration and summation over all allowed rotational levels, yields[3]

$$I(\pi/2) = \frac{\pi^2 c(\tilde{\nu}_{\text{in}} - \tilde{\nu}_p)^4}{2\varepsilon_0} N_i \mathscr{E}_0^2 \frac{45a^2 + 7\gamma^2}{45} \quad (33)$$

where we introduced the mean (isotropic) polarizability $a$:

$$a = \frac{1}{3}(\langle\alpha_{xx,fi}\rangle + \langle\alpha_{yy,fi}\rangle + \langle\alpha_{zz,fi}\rangle) \quad \left(\frac{\text{C m}^2}{\text{V}}\right) \quad (34)$$

and the anisotropy $\gamma$:

$$\gamma^2 = \frac{1}{2}[(\langle\alpha_{xx,fi}\rangle - \langle\alpha_{yy,fi}\rangle)^2 + (\langle\alpha_{yy,fi}\rangle - \langle\alpha_{zz,fi}\rangle)^2 + (\langle\alpha_{zz,fi}\rangle - \langle\alpha_{xx,fi}\rangle)^2 + 6(\langle\alpha_{xy,fi}\rangle^2 + \langle\alpha_{yz,fi}\rangle^2 + \langle\alpha_{zx,fi}\rangle^2)] \quad (\text{C}^2\text{m}^4\,\text{V}^{-2}) \quad (35)$$

Here, the classical polarizability tensor components have already been replaced by the quantum mechanical matrix elements. Introducing the irradiance $\mathscr{I}$

$$\mathscr{I} = \frac{1}{2}\varepsilon_0 c \mathscr{E}_0^2 \quad \left(\frac{\text{J}}{\text{s m}^2}\right) \quad (36)$$

we obtain with eq. (30) and the definitions

$$a'_p = \frac{1}{3}\{(\bar{\alpha}'_{xx})_p + (\bar{\alpha}'_{yy})_p + (\bar{\alpha}'_{zz})_p\} \quad (\text{C m kg}^{-1/2}\,\text{V}^{-1}) \quad (37)$$

$$\gamma'^2_p = \frac{1}{2}\{[(\bar{\alpha}'_{xx})_p - (\bar{\alpha}'_{yy})_p]^2 + [(\bar{\alpha}'_{yy})_p - (\bar{\alpha}'_{zz})_p]^2 + [(\bar{\alpha}'_{zz})_p - (\bar{\alpha}'_{xx})_p]^2 + 6[(\bar{\alpha}'_{xy})_p^2 + (\bar{\alpha}'_{yz})_p^2 + (\bar{\alpha}'_{zx})_p^2]\} \quad (\text{C}^2\,\text{m}^2\,\text{kg}^{-1}\,\text{V}^{-2}) \quad (38)$$

$$(\bar{\alpha}'_{rs})_p = \left(\frac{\partial\bar{\alpha}_{rs}}{\partial R_p^{(q)}}\right)_0 \quad (\text{C m kg}^{-1/2}\,\text{V}^{-1}) \quad (39)$$

the following expression for the intensity of a Stokes line:

$$I(\pi/2) = \frac{\pi^2}{\varepsilon_0^2}(\tilde{\nu}_{\text{in}} - \tilde{\nu}_p)^4 \mathscr{I} N_i(v_i^p + 1) b_{v_p}^2 \left(\frac{45a'^2_p + 7\gamma'^2_p}{45}\right) \quad \left(\frac{\text{J}}{\text{s sr}}\right) \quad (40)$$

Notice that $\gamma'^2_p$ and $\gamma^2$ are not directly related, but $\gamma'_p$ is related to $(\bar{\alpha}'_{rs})_p$ in the same way as $\gamma$ to $\langle\alpha_{rs,fi}\rangle$.

As it was already mentioned for the IR intensities, we have to sum the intensities over all levels of the normal mode $p$, because all transitions with $\delta v_p = 1$ occur at the same wave number (see ref. 3). This leads to the following expression for the Raman scattering intensity of a Stokes line:

$$I(\pi/2) = \frac{\pi^2}{\varepsilon_0^2}(\tilde{\nu}_{\text{in}} - \tilde{\nu}_p)^4 \mathscr{I} \frac{h}{8\pi^2 c\tilde{\nu}_p} \times \left(\frac{45a'^2_p + 7\gamma'^2_p}{45}\right) \frac{N_{\text{tot}}}{1 - \exp[-hc\tilde{\nu}_p/k_B T]} \quad \left(\frac{\text{J}}{\text{s sr}}\right) \quad (41)$$

The differential scattering cross section

$$\frac{d\sigma}{d\Omega} = \frac{I(\pi/2)}{\mathscr{I} N_{\text{tot}}} = \frac{\pi^2}{\varepsilon_0^2}(\tilde{\nu}_{\text{in}} - \tilde{\nu}_p)^4 \frac{h}{8\pi^2 c\tilde{\nu}_p} \times \left(\frac{45a'^2_p + 7\gamma'^2_p}{45}\right) \frac{1}{1 - \exp[-hc\tilde{\nu}_p/k_B T]} \quad \left(\frac{\text{m}^2}{\text{sr}}\right) \quad (42)$$

is often given instead of the intensity, because it is independent of the irradiance $\mathscr{I}$. Another possibility to express Raman intensities is the normalized differential cross section $d\sigma/d\Omega \cdot (\tilde{\nu}_{\text{in}} - \tilde{\nu}_p)^{-4}$, either as an absolute value or relative to the absolute value of the vibrational mode of $N_2$.[13] All these quantities depend on the experimental setup. Therefore, in many cases only the scattering factor (or Raman activity)

$$S = 45a'^2_p + 7\gamma'^2_p \quad \left(\frac{\text{C}^2\,\text{m}^2}{\text{amu V}^2}\right) \quad (43)$$

is calculated by quantum chemistry programs, because this is a pure molecular property and independent of experimental setup. It is usually given in unit (Å$^4$/amu),** which follows from the use of the polarizability volume $\alpha_V = a/(4\pi\varepsilon_0)$, which has the unit of volume, Å$^3$. In other cases, these scattering factors are multiplied by the value of $b_{v_p}$, eq. (28), in order to obtain parameters in the SI units of the polarizability, Cm$^2$/V.

## Efficient Calculation of Derivatives

The second derivatives of the electronic energies, eq. (2), can be obtained as numerical first derivatives of the analytically determined gradient (see the next section). Similarly, the derivatives of dipole moments, eq. (29), and polarizabilities, eq. (30), can be obtained by numerical differentiation. Gradients, dipole moments, and polarizabilities have to be calculated for several different distorted structures to determine the numerical derivatives according to a central difference formula. If a 3-point central differences Bickley formula[14] is used, the data must be calculated for $6N$

**Note that amu is not the mass unit in atomic units but the so-called (unified) atomic mass unit, which is sometimes denoted as $u = (1/12)m(^{12}\text{C}) = 10^{-3}\,\text{kg mol}^{-1}/N_A$.

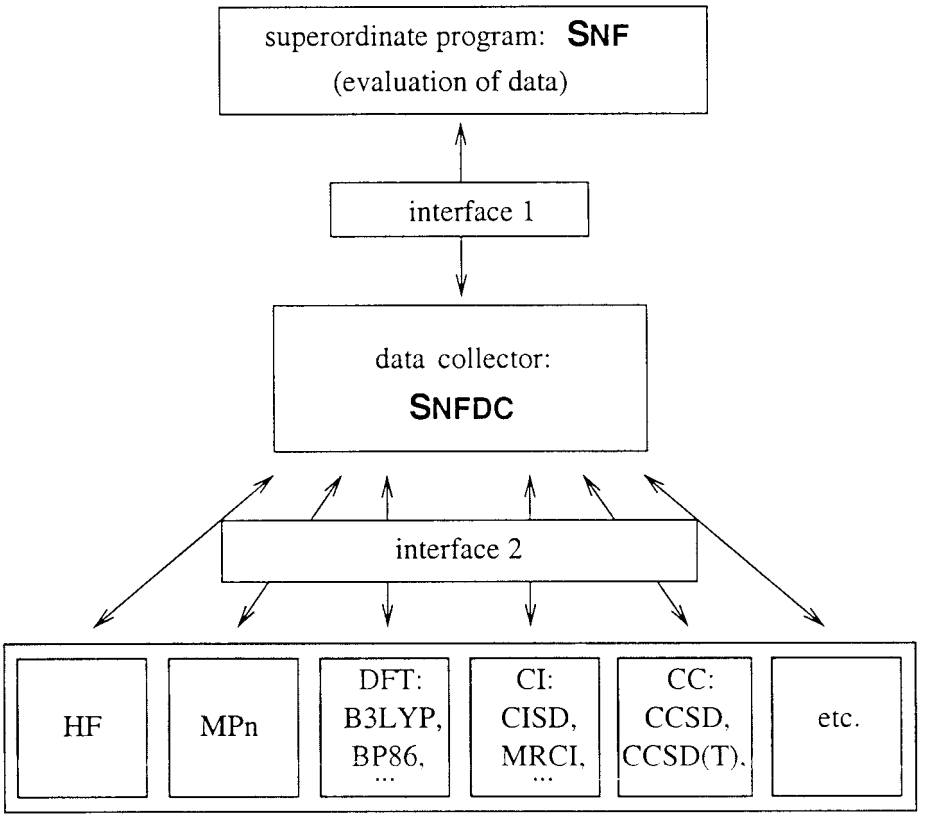


**Figure 1.** Hierarchical structure of programs for a frequency calculation.

different structures of the molecule, because every atomic Cartesian coordinate has to be distorted in positive and negative direction. It is desirable to reduce the computational effort by taking advantage of the molecular point group symmetry. Only those distorted structures must be calculated, which require displacements for a minimal set of symmetry nonredundant atoms. The other data may be obtained from these calculations by the use of the symmetry operations.

If the molecule exhibits a nontrivial point group symmetry, symmetry operations of this point group map the position of one nucleus $A_1$ onto the position of another nucleus $A_2$. The operators for symmetry operations $S$ are represented by matrices $\mathbf{D}_S^{(c)}$ in a basis of Cartesian distortion coordinates. By performing the calculation for all displacements of the coordinates of atom $A_1$, we get the dipole moments, polarizabilities, and gradients for the displacements of the coordinates of atom $A_2$ by

$$\mu^{(c)}(2) = \mathbf{D}_S^{(c)}\mu^{(c)}(1), \quad \alpha^{(c)}(2) = \mathbf{D}_S^{(c)}\alpha^{(c)}(1)\mathbf{D}_S^{(c)\dagger},$$
$$\nabla E(2) = \mathbf{D}_S^{(c)}\nabla E(1) \quad (44)$$

With these transformations we obtain for the derivatives

$$\nabla^{(c)}(2)\mu^{(c)}(2) = \mathbf{D}_S^{(c)}\nabla^{(c)}(1)\mu^{(c)}(2),$$
$$\nabla^{(c)}(2)\alpha^{(c)}(2) = \mathbf{D}_S^{(c)}\nabla^{(c)}(1)\alpha^{(c)}(2) \quad (45)$$

and for the corresponding part of the Hessian

$$\mathbf{F}^{(c)}(2) = \mathbf{D}_S^{(c)}\mathbf{F}^{(c)}(1)\mathbf{D}_S^{(c)\dagger} \quad (46)$$

In order to obtain the energy eigenvalues $\varepsilon_p$ it is necessary to diagonalize the Cartesian Hessian matrix $\mathbf{F}^{(c)}$ after mass-weighting to obtain the matrix $\mathbf{F}^{(q)}$:

$$\mathbf{F}^{(q)} = \mathbf{U}^{(m)\dagger}\mathbf{F}^{(m)}\mathbf{U}^{(m)} = \mathbf{U}^{(m)\dagger}\mathbf{M}^{-1/2}\mathbf{F}^{(c)}\mathbf{M}^{-1/2}\mathbf{U}^{(m)} \quad (47)$$

where $\mathbf{F}^{(m)}$ denotes the mass-weighted Hessian matrix and $\mathbf{M}^{-1}$ is a diagonal matrix, which contains $M_{ij}^{-1} = \delta_{ij}/m_i$. The nuclear mass $m_i$ is the mass of the atom corresponding to the Cartesian coordinate $R_i^{(c)}$. Standard projection operators

$$\mathbf{P}_\mu^{(c)} = \frac{n_\mu}{h}\sum_{S=1}^{h}\chi_{S,\mu}^{*}\mathbf{D}_S^{(c)} \quad (48)$$

where $\chi_{S,\mu}$ is the character of $S$ in the irreducible representation (irrep) $\Gamma_\mu$ of dimension $n_\nu$ ($h$ is the order of the group), can be applied to obtain a block diagonalized Hessian. By diagonalizing the projection operator we obtain the matrix of eigenvectors $\mathbf{S}_\mu^{(c)}$:

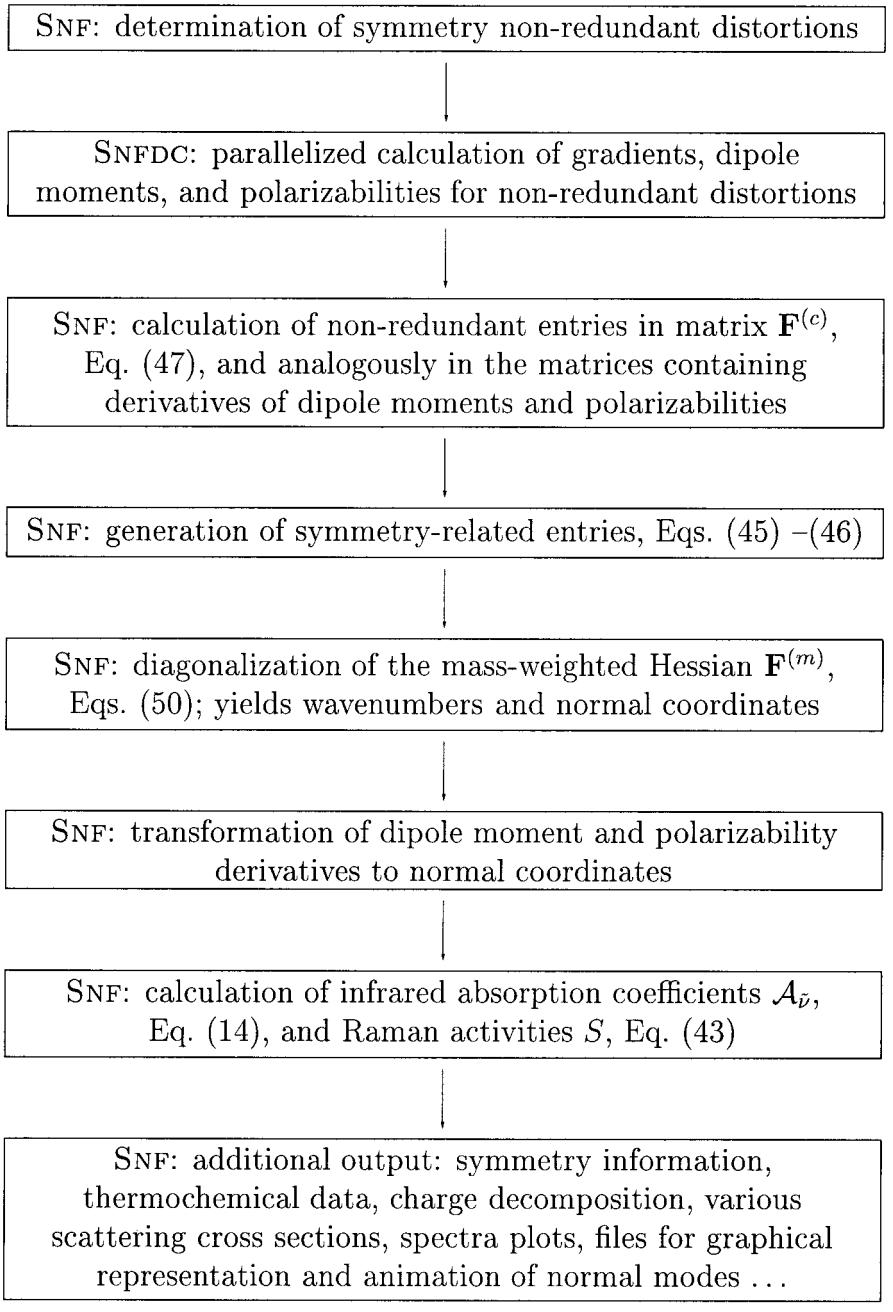


**Figure 2.** Flow chart of the calculation of vibrational spectra using a superordinate program (SNF) and a data collector (SNFDC).

$$\mathbf{S}_{\mu}^{(c)\dagger}\mathbf{P}_{\mu}^{(c)}\mathbf{S}_{\mu}^{(c)} = \mathbf{P}_{\mu}^{(s)} \tag{49}$$

which may be used in turn to get the Hessian for irrep $\Gamma_\mu$ in the symmetry adapted basis:

$$\mathbf{S}_{\mu}^{(c)\dagger}\mathbf{F}^{(m)}\mathbf{S}_{\mu}^{(c)} = \mathbf{F}_{\mu}^{(s)} \tag{50}$$

Here we used the fact that mass-weighting of the Cartesian coordinates affects neither $\mathbf{P}_{\mu}^{(c)}$ nor $\mathbf{S}_{\mu}^{(c)}$, so that $\mathbf{S}_{\mu}^{(c)} = \mathbf{S}_{\mu}^{(m)}$. Each block $\mathbf{F}_{\mu}^{(s)}$ can now be diagonalized separately. Most important is that the use of projection operators allows us to classify the vibrations according to the irreps of the point group.

At this stage, the Hessian still contains contributions for rotations and translations. In principle, these modes should have a zero vibrational frequency, because the electronic energy, that is, the potential in which the nuclei move, is not affected by these motions. However, these types of motion show absolute values of the frequencies, which are slightly larger than zero in absolute

**Table 1.** Static and Dynamic Raman Scattering Activities (Å$^4$/amu) for Methane.

| Irrep | Method basis $\tilde{\nu}$ | BP86 TZVP static | BP86 TZVPP static | BP86 Sadlej static | BP86 TZVext static | SCF Sadlej static | B3LYP Sadlej static |
|---|---|---|---|---|---|---|---|
| $t_2$ | 1302.52 | 4.26 | 1.03 | 0.33 | 0.14 | 0.11 | 0.33 |
| $e$ | 1518.86 | 51.61 | 31.23 | 9.30 | 5.34 | 8.66 | 9.12 |
| $a_1$ | 2972.48 | 166.26 | 181.18 | 248.05 | 228.94 | 236.22 | 238.62 |
| $t_2$ | 3083.71 | 180.25 | 158.89 | 147.57 | 142.24 | 153.14 | 146.72 |

| Irrep | Method basis $\tilde{\nu}$ | SCF Sadlej dyn. | BP86 Sadlej dyn. | B3LYP Sadlej dyn. | SCF[23] Sadlej dyn. | B3LYP[23] Sadlej dyn. | Exp.[34] (488 nm) |
|---|---|---|---|---|---|---|---|
| $t_2$ | 1302.52 | 0.22 | 0.68 | 0.64 | 0.20 | 0.83 | $\leq$0.24 |
| $e$ | 1518.86 | 8.71 | 8.94 | 8.86 | 8.82 | 9.2 | 7.0 $\pm$ 0.4 |
| $a_1$ | 2972.48 | 261.47 | 280.98 | 268.45 | 260.24 | 268.24 | 230 $\pm$ 12 |
| $t_2$ | 3083.71 | 174.44 | 172.85 | 170.55 | 173.00 | 168.00 | 128 $\pm$ 7 |

Vibrational wave numbers $\tilde{\nu}$ (BP86/TZVP) in cm$^{-1}$. Dynamic values were calculated for an incident beam of wavelength $\lambda$ = 514.5 nm in order to make the results comparable to the data by Van Caillie and Amos.[23]

value due to errors in the numerical differentiation procedure. Two techniques may be useful to eliminate the rotational and translational modes to avoid mixing with vibrational modes. The first option is to determine the percentage of translational and vibrational contributions to a normal mode by comparing the resulting momentum and angular momentum of the normalized mode with the corresponding values for a normalized translational and rotational mode. For a pure vibrational normal mode, a zero momentum and angular momentum must occur. The modes with the three largest translational and rotational percentages may be eliminated.

The second option is to perform this elimination before the diagonalization of the Hessian matrix. This has the advantage that coupling of translational and rotational with vibrational modes due to numerical inaccuracy can be avoided. Because it is possible to construct idealized translational and rotational normal modes, these motions can be eliminated by applying projection operators.[15] In our implementation, both methods are applied and their results are used for internal consistency checks.

## Program Design

The formalism for the calculation of vibrational spectra, which we presented in the preceding sections, is only useful in practice if efficient computer codes can be designed for the solution of the relevant equations. Features and structure of such a program package should fulfill certain requirements in order to allow for fast analyses of large molecules. The primary data to be calculated are first (analytical) derivatives of the electronic energy for the vibrational wave numbers and normal modes, dipole moments for the IR intensities, and polarizability tensors for the Raman intensities. In particular, the following points should be considered.

Because a lot of complex quantum chemical methods (e.g., Hartree-Fock, density functional theory, Møller-Plesset perturbation theory, configuration interaction, or coupled cluster methods)

**Table 2.** Static Raman Scattering Activities (Å$^4$/amu) for $C_{20}^{2+}$ (DFT/BP86).

| Irrep | $\tilde{\nu}$ | TZVP | TZVext | Sadlej |
|---|---|---|---|---|
| $h_g$ | 504.04 | 111.3476 | 112.0559 | 111.4018 |
| $a_g$ | 823.99 | 129.1219 | 127.3905 | 127.6018 |
| $h_g$ | 1123.70 | 14.6487 | 15.8161 | 17.2595 |
| $h_g$ | 1371.10 | 51.7958 | 45.0298 | 44.6925 |

Vibrational wave numbers $\tilde{\nu}$ (BP86/TZVP) in cm$^{-1}$.

**Table 3.** Polarizability Volumes $\alpha_V$ (bohr$^3$) for Benzene Using Different Basis Sets (DFT/BP86).

| Basis set | # basis fcts. | $\alpha_V$ |
|---|---|---|
| TZVP | 150 | 65.33 |
| TZVP + *s*(1.0) | 151 | 65.60 |
| TZVP + *sp*(1.0) | 154 | 67.15 |
| TZVP + *spd*(1.0) | 159 | 67.42 |
| TZVP + *spdf*(1.0) | 166 | 67.62 |
| TZVP + *s*(1.2) | 151 | 65.66 |
| TZVP + *sp*(1.2) | 154 | 67.83 |
| TZVP + *spd*(1.2) | 159 | 68.48 |
| TZVP + *spdf*(1.2) | 166 | 68.81 |
| TZVP + *s*(1.5) | 151 | 65.64 |
| TZVP + *sp*(1.5) | 154 | 66.60 |
| TZVP + *spd*(1.5) | 159 | 67.42 |
| TZVP + *spdf*(1.5) | 166 | 68.62 |
| TZVext | 198 | 70.84 |
| Sadlej | 198 | 72.24 |
| CCSD/Sadlej[41] | 198 | 69.17 |
| Exp.[42] | | 68.53 |

The numbers in parentheses in the first column are the scale factors for $r_{max}$; compare the discussion in the section "Basis Set Dependencies."

**Table 4.** Polarizability Volumes $\alpha_V$ (bohr$^3$) for $C_{60}$ Using Different Basis Sets (DFT/BP86).

| Basis set | # Basis fcts. | $\alpha_V$ |
|---|---|---|
| TZVP | 1140 | 549.6 |
| TZVP + *spdf*(1.15) | 1156 | 553.9 |
| TZVext | 1440 | 561.4 |
| CRPA,[43] 4-31(p,d) | 1020 | 579 |
| Exp.[44] | | 596 |

Experimental value calculated from refractive index.

and program packages are available, it is not desirable to care about solving the particular electronic Schrödinger equation (in SCF or RPA form). This can easily be done by the existing programs. Only their output files should be processed, because extending existing programs may destroy their algorithmic structure and affect their elegance, transparency, and efficiency.

These quantum chemistry programs usually provide the gradient of the total electronic energy, which is needed for structure optimization. In contrast to this, by far not all programs are able to calculate analytic second derivatives of the electronic energy, and even if this feature is included in a package, it may cause difficulties for large molecules or certain quantum chemical methods. In order to keep the frequency analysis program as universal as possible, the second derivatives may be calculated by numerical differentiation of analytically determined gradients of the total electronic energy.

Well-defined interfaces are necessary in order to use independent source codes for the solution of the electronic Schrödinger equation and for the frequency analysis in order to maintain a concise structure.

Additionally, matrix elements of dipole moments and (static as well as dynamic) polarizability tensors must be computed with an external program to be used for intensity calculations. Many programs are able to provide these data, and so the superordinate frequency analysis program can easily be extended. Because the derivatives of these data with respect to the normal coordinates are of interest, numerical differentiation is also applied here. To be sure, methods to calculate analytical derivatives of dipole moments and polarizabilities for *standard* methods like HF are well known[16–18] and implemented.

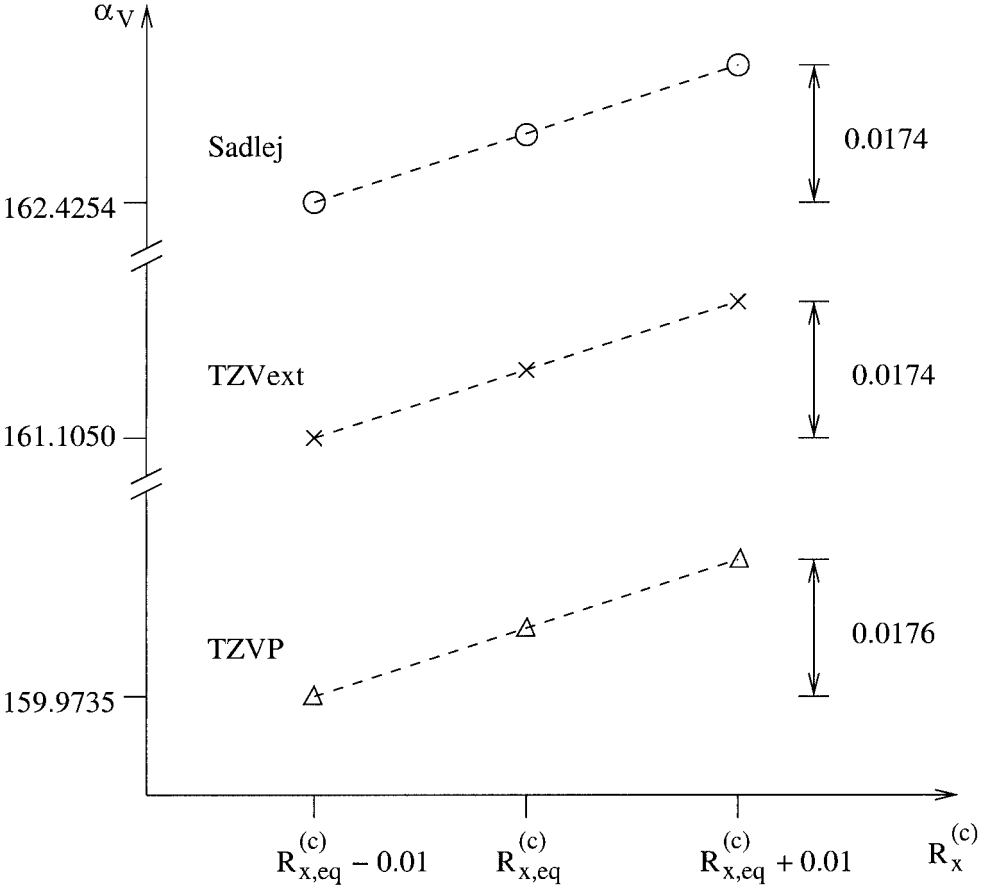


**Figure 3.** Variation of the mean polarizability volume $\alpha_V$ (bohr$^3$) of $C_{20}^{2+}$ with respect to a distortion in the $R_x^c$ coordinate (bohr) of a carbon atom for different basis sets.

The derivatives are often carried out as numerical or analytical derivatives of the gradient with respect to a static external electric field, because we have, according to the Hellmann-Feynman theorem[19]

$$\bar{\mu}_q = -\left(\frac{d\bar{E}_{\mathrm{el}}}{d\,\mathscr{E}_q}\right)_0, \quad \bar{\alpha}_{qp} = -\left(\frac{d^2\bar{E}_{\mathrm{el}}}{d\,\mathscr{E}_q d\,\mathscr{E}_p}\right)_0, \quad p, q = \{x, y, z\} \tag{51}$$

For other methods, the derivative calculations are performed numerically[20] (finite field techniques), as introduced by Komornicki and McIver.[21] Neither treatment is able to consider the frequency-dependence of the polarizability, because they regard only the effect of a static electric field on molecular properties. In order to evaluate also Raman intensities with dynamic polarizabilities, it is necessary to calculate these frequency-dependent properties and to subsequently differentiate them with respect to the normal coordinates. No analytical implementation is available for this task, but the neglect of the frequency-dependence causes effects that are comparable to the effects from the neglect of electron correlation.[22,23] Numerical differentiation makes it possible to allow for dynamical polarizabilities.

Numerical differentiation with respect to nuclear coordinates requires the calculation of the gradient, dipole moment, and polarizability tensor for several different structures, in which single nuclear coordinates are displaced compared to the equilibrium structure. The superordinate program itself controls the execution of these single-point calculations and evaluates the data that have been stored by a data collector. The accuracy of the frequency calculation can systematically be improved by using a 5-point (etc.) central differences Bickley formula.[14]

Major advantages for practical use of the implementation can be achieved by the following features. Because single-point calculations may become computationally expensive if large molecules are considered, the full point group symmetry of the molecule can be exploited a priori in order to keep the number of mandatory single-point calculations as small as possible (see "Efficient Calculation of Derivatives"). Furthermore, it is desirable to use a parallel implementation for the frequency analysis, such that different single-point calculations can be done on different nodes of a computer cluster. Additionally, a fine-grained parallelization of the single-point calculations is possible if the quantum chemistry program package itself, which is utilized for this purpose, is able to run parallelized.

A hierarchical structure of the program design, which we use to achieve the features mentioned above, is shown in Figure 1.

For the calculation of vibrational spectra, we have developed the superordinate program SNF,[24††] which is able to perform a calculation of vibrational wave numbers, IR, and Raman intensities, taking advantage of the point group symmetry of the molecule. A flow chart of this program is given in Figure 2. For a coarse-grained parallelized data collection, SNF utilizes its data collector SNFDC.[25] In their present versions, the quantum chemistry packages TURBOMOLE[26] and DALTON[27] can be used for the generation of primary data.

††For a detailed technical description of the program see ref. 15. The program can be obtained from the authors.

**Table 5.** Vibrational Wave Numbers $\tilde{\nu}$ (BP86/TZVP) and $\tilde{\nu}^{\mathrm{exp}}$ (1/cm), Infrared Absorption Coefficients $\mathscr{A}_{\tilde{\nu}}$ ($10^5$ cm/mol), and Raman Scattering Factors $S$ (Å$^4$/amu) for $C_{60}$.

| No. | Irrep | $\tilde{\nu}$ | $\tilde{\nu}^{\mathrm{exp37}}$ | $\mathscr{A}_{\tilde{\nu}}$ | $S$ |
|---|---|---|---|---|---|
| 1–5 | $H_g$ | 254.79 | 273 | | 25.40 |
| 6–9 | $T_{2u}$ | 334 | | | |
| 9–12 | $F_u$ | 342 | | | |
| 13–17 | $H_u$ | 397 | | | |
| 18–22 | $H_g$ | 424 | 437 | | 0.43 |
| 23–26 | $F_g$ | 472 | | | |
| 27 | $A_g$ | 479 | 496 | | 189.95 |
| 28–32 | $H_u$ | 524 | | | |
| 33–35 | $T_{1u}$ | 528 | 527 | 22.04 | |
| 36–38 | $T_{2g}$ | 545 | | | |
| 39–41 | $T_{1g}$ | 559 | | | |
| 42–45 | $F_g$ | 562 | | | |
| 46–48 | $T_{1u}$ | 573 | 577 | 18.74 | |
| 49–53 | $H_u$ | 654 | | | |
| 54–56 | $T_{2g}$ | 685 | | | |
| 57–61 | $H_g$ | 699 | 710 | | 0.03 |
| 62–64 | $T_{2u}$ | 708 | | | |
| 65–69 | $H_u$ | 721 | | | |
| 70–73 | $F_u$ | 724 | | | |
| 74–77 | $F_g$ | 743 | | | |
| 78–81 | $F_u$ | 745 | | | |
| 82–86 | $H_g$ | 769 | 774 | | 14.58 |
| 87–89 | $T_{2g}$ | 781 | | | |
| 90–92 | $T_{1g}$ | 804 | | | |
| 93 | $A_u$ | 896 | | | |
| 94–97 | $F_u$ | 956 | | | |
| 98–100 | $T_{2u}$ | 962 | | | |
| 101–104 | $F_g$ | 1074 | | | |
| 105–109 | $H_g$ | 1096 | 1099 | | 14.06 |
| 110–112 | $T_{2u}$ | 1177 | | | |
| 113–115 | $T_{1u}$ | 1180 | 1183 | 6.82 | |
| 116–120 | $H_u$ | 1203 | | | |
| 121–125 | $H_g$ | 1234 | 1250 | | 21.86 |
| 126–128 | $T_{1g}$ | 1258 | | | |
| 129–132 | $F_u$ | 1290 | | | |
| 133–136 | $F_g$ | 1295 | | | |
| 137–139 | $T_{2g}$ | 1315 | | | |
| 140–144 | $H_u$ | 1322 | | | |
| 145–149 | $H_g$ | 1412 | 1428 | | 1.19 |
| 150–153 | $F_u$ | 1414 | | | |
| 154–156 | $T_{1u}$ | 1425 | 1428 | 10.01 | |
| 157 | $A_g$ | 1467 | 1470 | | 401.30 |
| 158–161 | $F_g$ | 1484 | | | |
| 162–164 | $T_{2u}$ | 1516 | | | |
| 165–169 | $H_u$ | 1545 | | | |
| 170–174 | $H_g$ | 1555 | 1575 | | 55.67 |

$\mathscr{A}_{\tilde{\nu}}$ and $S$ are only given for infrared and Raman active modes.

## Example: Buckminsterfullerene $C_{60}$

In order to demonstrate the efficiency of our implementation, we present vibrational spectra for the highly symmetric Buckminsterfullerene $C_{60}$. Our emphasis is on the accurate calculation of Raman intensities, because it has not yet been possible to calculate reliable Raman spectra.

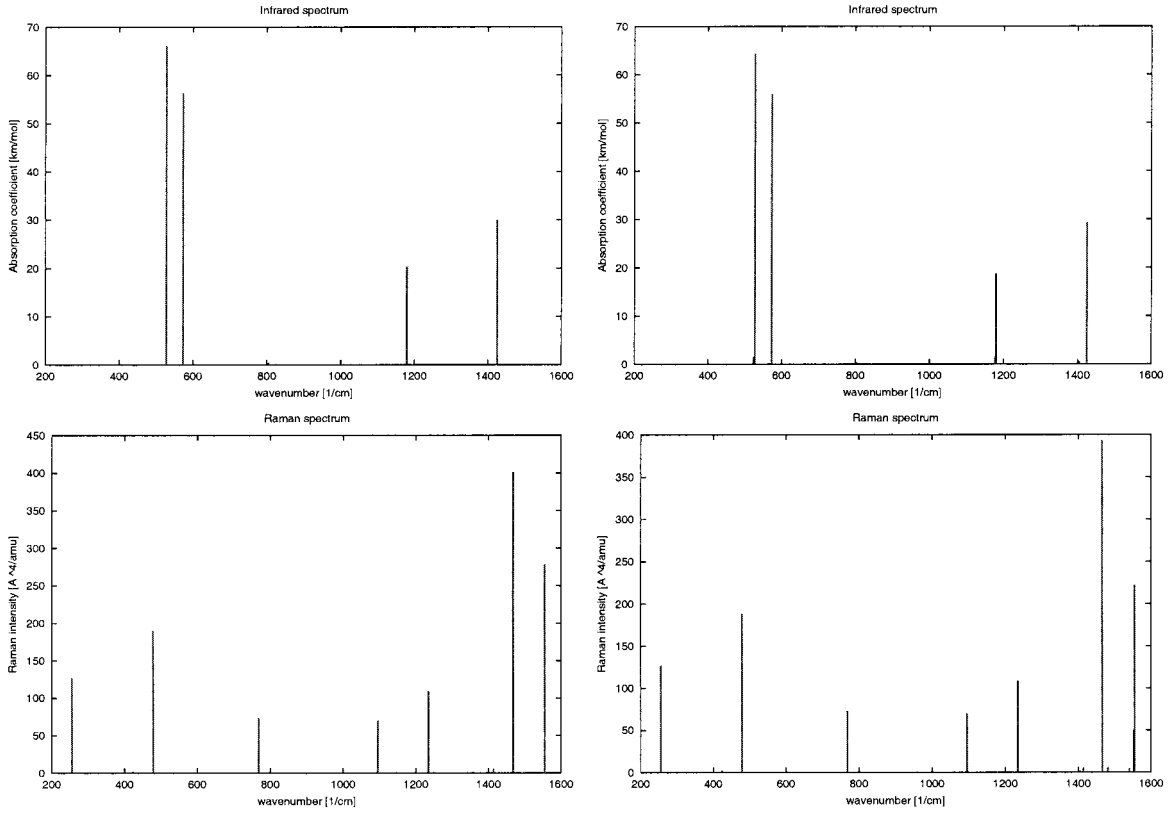


**Figure 4.** Infrared (top) and Raman (bottom) line spectra for $C_{60}$ (left) and $C_{60}$ containing one $^{13}C$ atom (right).

### *Basis Set Dependencies*

Polarizabilities show a much stronger dependence on the chosen basis set than other molecular properties like total electronic energies. However, better polarizabilities do not necessarily guarantee improved Raman intensities, because they depend on differences of polarizabilities if numerical differentiation with respect to nuclear coordinates is used.

To test the influence of the basis set on the results obtained, we performed calculations for $CH_4$ and used the TZVP and TZVPP[28] basis sets as well as the one introduced by Sadlej,[29] which is a frequently used basis set for the calculation of molecular electric properties.[22,23,30–32] Although the latter basis set is very efficient for the prediction of polarizabilities and Raman intensities,[33] equilibrium structures and vibrational wave numbers can be worse than those calculated with, for instance, the TZVP basis set. The frequencies obtained with this basis set in combination with density functional methods are in most cases in good agreement with experiment, such that a scaling of the frequencies is not applied.[‡‡] Therefore, we combined the TZV kernel (i.e., the TZVP basis without the *d* function for carbon and without the *p* function for hydrogen) with the two contracted *d*- and *p*-types, respectively, polarization functions of the Sadlej basis (in the following dubbed as TZVext). This leads to a total number of 60 basis functions for carbon, which is the same number of functions as in the case of the Sadlej basis. We found that the TZVext basis gives better vibrational frequencies in some cases. All data for $CH_4$ given in Table 1 were calculated using the BP86 exchange correlation functional for static and dynamic polarizabilities.

Compared to the experimental values,[34] we obtained better results for Raman intensities with our extended basis set TZVext than with the Sadlej basis, while the minimum structure and the vibrational wave numbers were of the same quality as the results found with the TZVP basis set.

The Raman intensities obtained with the TZVP basis set are unsatisfactory in this case and differ qualitatively from the experimental values. The additional polarization functions in the TZVPP basis lead only to a slight improvement, while both TZVext and Sadlej basis sets give better results because they contain additional diffuse polarization functions. However, these diffuse functions can cause convergence problems for large molecules such that a calculation for $C_{60}$ with TZVext becomes unfeasible. In symmetric and compact molecules like $C_{60}$ the effect of these additional diffuse functions might be smaller because polarization functions from neighboring centers may model the effect of diffuse functions.

[‡‡]Note also that scaling of frequencies in order to reproduce experimental data is not always desirable as it would blur the accuracy of the approximations involved in the calculation of the intensities, which are reviewed in detail in this work.

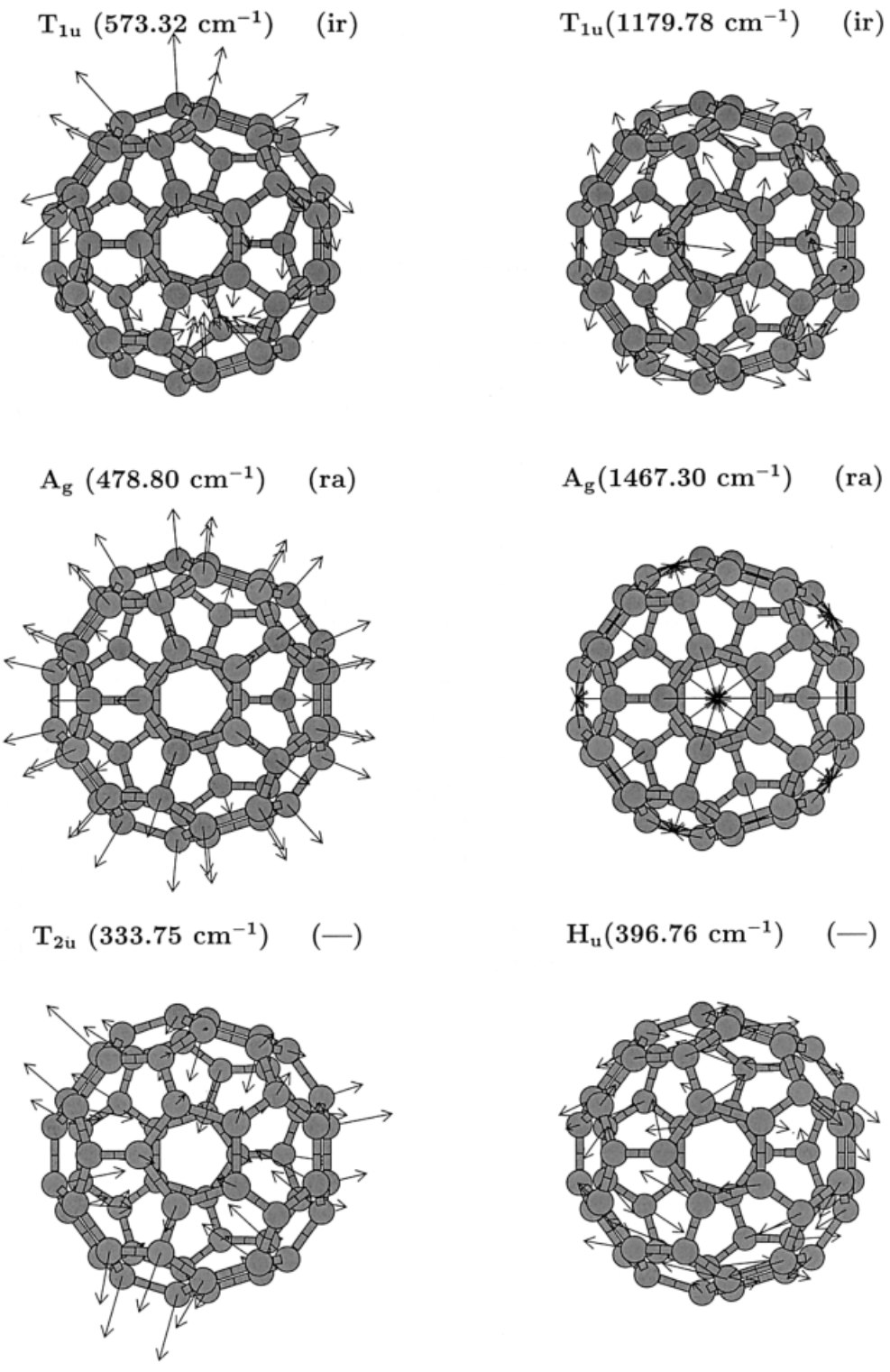


**Figure 5.** Selected normal modes for $C_{60}$: (ir) = infrared active, (ra) = Raman active, (−) infrared and Raman inactive.

Instead of $CH_4$ we chose the icosahedral closed-shell molecule $C_{20}^{2+}$ as a suitable model for Buckminsterfullerene. In this case, the Raman intensities calculated with TZVP, TZVext, and the Sadlej basis, which are given in Table 2, compare well, indicating that the TZVP basis set is sufficiently large for the calculation of the Raman spectrum of $C_{60}$.

A change from the TZVP to the Sadlej or the TZVext basis set raises the number of basis functions for $C_{60}$ from 1140 to 1440, which drastically increases the computational effort, such that the single-point calculations in $C_1$ symmetry are no longer feasible. If a better description of the polarizability for the molecule is necessary, but the use of larger basis sets is not possible, one may use additional basis functions at a dummy atom in the center of the molecule. We tested the influence of these additional basis functions on the polarizabilities for benzene and $C_{60}$. The exponents for the GTO functions were obtained such that the radial density of the functions has its maximum at the position of the carbon atoms or at slightly larger values. The relationship between the maximum of the radial density and the exponent $\alpha_{n,l}$ is given by

$$\alpha_{n,l} = \frac{l+1}{2r_{\max}^2} \tag{52}$$

With basis functions obtained in this way, we performed calculations for benzene. We used the values $r_{\max} = 2.643$ and $r_{\max} = 2.643 \cdot a$ bohr, with $a = 1.2$ and $a = 1.5$, that is, radii increased by 20 and 50%, to calculate the polarizabilities of the benzene molecule. The results are presented in Table 3. The accuracy obtained with an additional set of *spdf* functions in the center of the benzene ring is comparable or even better than that of the Sadlej or TZVext basis set. The best results were obtained for the value $r_{\max} = 2.643 \cdot 1.2$ bohr. Although the influence on the polarizabilities is rather large, the dummy-centered basis functions do not improve the Raman intensities, where the derivatives of the polarizabilities enter.

For the polarizability calculations of $C_{60}$, we used the value $r_{\max} = 6.718 \cdot 1.15$ bohr to determine the optimum exponents for dummy-centered basis functions. The resulting data are given in Table 4. In this case, the polarizabilities are not as well described by the TZVP + *spdf* basis as by the TZVext basis.

In order to test whether reliable Raman intensities can be obtained in cases where the polarizability itself is not well reproduced, we plotted in Figure 3 the variation of the mean polarizability volume $\alpha_v$ of $C_{20}^{2+}$ with respect to distortions of a nuclear coordinate of a carbon atom. The differences in the polarizabilities for different basis sets are very large compared to the differences that are used to calculate the Raman intensities. Although the mean polarizabilities $\alpha_V$ for this molecule differ by about 2.5 bohr$^3$ between the TZVP and the Sadlej basis set, the variation in $\alpha_V$ with respect to a distortion of the nuclear coordinates, which is about 0.0175 bohr$^3$ for a step size of 0.01 bohr in the numerical differentiation, is almost equal for these basis sets.

From these tests it is clear that the accuracy of the Raman intensities for the fullerene $C_{60}$ is well described by a TZVP basis set due to the error cancellation in the numerical differentiation. The accuracy of the polarizability does not allow us to draw conclusions on the accuracy of the numerically calculated Raman intensities.

To summarize, the quality of the calculated Raman intensities is promising, which indicates that all the approximations are legitimate. However, this may partly be ascribed to error compensation, because the consideration of the frequency-dependence of the polarizability often impairs the agreement with the experimental results.

### *Raman Spectrum of $C_{60}$*

The Buckminsterfullerene $C_{60}$ is an ideal example to demonstrate the powerful features of the algorithmic design described in the section "Program Design." Because it contains 60 atoms, at least 360 single-point calculations would be necessary to determine the vibrational spectra. Taking advantage of the molecular symmetry (point group $I_h$), we only need to calculate six displacement geometries for one single carbon atom, because all atoms are symmetrically equivalent. This reduces the total CPU time by a factor of 60. It allows us to perform the first reliable fully quantum chemical calculation of the Raman spectrum of $C_{60}$.

For $C_{60}$ we used the program package TURBOMOLE[26] to carry out the single-point calculations of the molecular properties for all displacement structures. Because the distortions destroy the symmetry of the molecule, all single-point calculations were carried out in $C_1$ symmetry. We studied the molecule using DFT methods with the BP86 exchange-correlation functional[35,36] and the TZVP basis set.[28]

A calculation for the six displacement geometries, including the determination of the polarizabilities, took about 14 days of CPU time on six Linux-PCs with 900 MHz AMD-Athlon CPUs. The wall time for the whole calculation without utilizing molecular symmetry and parallelization would have been more than 14 years on a single processor machine.

The vibrational wave numbers, the absorption coefficients for the IR spectra calculated [note that the coefficients $\mathcal{A}_{\bar{\nu}}$ from eq. (14) are given], and the Raman scattering factors according to eq. (43) can be found in Table 5. Note that we refrain from comparison with experimental results from ref. 37 for the Raman intensities because these experimental values are not directly comparable to our results, for three reasons: the wavelength of the laser beam lies in the area of electronic excitations of $C_{60}$ enforcing the framework of *resonance* Raman theory (see, e.g., refs. 3 and 38); the spectrum was measured in *condensed* phase (film samples); and finally, relative intensities are given in ref. 37 instead of Raman activities such that more details concerning the experimental setup seem to be necessary. The latter two arguments also hold for other studies that have tried to circumvent the problem of the resonance Raman effect.[39,40] All wave numbers agree very well with the experimental values; the maximum differences are only about 20 cm$^{-1}$.

From the character table of the point group $I_h$ it can be seen that within the harmonic approximation only vibrations of the irrep $T_{1u}$ should yield nonzero IR intensities, while vibrations of the irreps $A_g$ and $H_g$ should be Raman active according to the exclusion principle, valid for point groups with centers of inversion. This is easily verified from Table 5. In Figure 4 the IR and Raman line spectra for $C_{60}$ are presented.

Figure 5 shows schematically six of the 174 vibrational normal modes in terms of the displacement vectors. Two of them show IR activity, two Raman activity, and two cannot be detected either in IR or in Raman spectroscopy.

Once the electronic energy is known for several points on the potential energy surface, isotope effects can easily be studied. The electronic energy is—within the Born-Oppenheimer approximation—independent of the nuclear masses. Isotope effects may be explored by just setting up a modified matrix $\mathbf{M}^{-1/2}$ in eq. (47), which contains the masses of the selected isotopes, without rerunning the data collector. Figure 4 also shows the IR and Raman spectra calculated for a $C_{60}$ molecule containing one $^{13}C$ atom. This is of interest, because the probability for a composition of $C_{60}$ with one $^{13}C$ isotope is about 34%.

Although the isotope effect is not very large, it can clearly be seen that additional lines occur in both spectra due to symmetry breaking. In the IR spectrum, new peaks with low intensities can be found at 524, 1177, and 1405 $cm^{-1}$, and in the Raman spectrum at 1481, 1540, and 1553 $cm^{-1}$.

The remarkable accuracy of the wave numbers leads us to search for possible error cancellation. Effort is now being undertaken to calculate anharmonicities in order to test the mechanical harmonic approximation.

## Conclusions

In this work it has been shown how an efficient calculation of vibrational spectra for large molecules can be achieved within the double harmonic approximation, emphasizing the applied approximations and conditions for their validity. The use of numerical derivatives of gradients, dipole moments, and polarizability tensors allows us to use a wide variety of quantum chemical program packages for the single-point calculations and makes a powerful coarse-grained parallelization straightforward. Fine-grained parallelization can additionally be used if this feature is available in the applied program packages for the solution of the electronic Schrödinger equation. Numerical derivatives are today the only choice if frequency-dependent polarizabilities shall be calculated to predict the Raman intensities.

The well-defined interfaces permit a clear separation of different hierarchical levels in the calculation and make an extension to new methods very easy.

Taking advantage of the molecular point group symmetry reduces the computational costs and increases the accuracy of the results. As an example we presented a vibrational analysis of the Buckminsterfullerene $C_{60}$, for which we calculated the first reliable quantum chemical vibrational spectra.

## Acknowledgments

J. N. gratefully acknowledges funding by a Kekulé-Stipendium of the Fonds der Chemischen Industrie.

## References

1. Herzberg, G. Molecular Spectra and Molecular Structure II. Infrared and Raman Spectra of Polyatomic Molecules; Van Nostrand Reinhold: New York, 1945.
2. Wilson, E. B.; Decius, J. C.; Cross, P. C. Molecular Vibrations; McGraw-Hill: New York, 1955.
3. Long, D. A. Raman Spectroscopy; McGraw-Hill: New York, 1977, pp. 31, 81–82.
4. Pugh, L. A.; Rao, K. N. In Molecular Spectroscopy: Modern Research, Vol. II; Academic Press: New York, 1976, p. 165.
5. Galabov, B. S.; Dudev, T. Vibrational Intensities; Elsevier: Amsterdam, 1996.
6. Cioslowski, J. J Am Chem Soc 1989, 111, 8333.
7. Heitler, W. The Quantum Theory of Radiation; Dover: New York, 1994, p. 136.
8. Craig, D. P.; Thirunamachandran, T. Molecular Quantum Electrodynamics; Dover: New York, 1998, pp. 17, 84, 89.
9. Overend, J. In Infra-Red Spectroscopy and Molecular Structure; Davies, M., Ed.; Elsevier: Amsterdam, 1963, p. 345.
10. McQuarrie, D. A.; Simon, J. D. Molecular Thermodynamics; University Science Books: Sausalito, 1999, p. 105.
11. Placzek, G. Z Physik 1931, 70, 84.
12. Rose, M. E. Elementary Theory of Angular Momentum; Wiley: New York, 1957.
13. Schrötter, H. W.; Klöckner, H. W. In Raman Spectroscopy of Gases and Liquids; Weber, A., Ed.; Springer: Berlin, 1979, p. 123.
14. Bickley, W. G. Math Gaz 1941, 25, 19.
15. Neugebauer, J. SNF Program Manual; University of Erlangen-Nürnberg: 2002.
16. Yamaguchi, Y.; Frisch, M.; Gaw, J.; Schaefer HF, III.; Stephen Binkley, J. J Chem Phys 1986, 84, 2262.
17. Yamaguchi, Y.; Frisch, M.; Gaw, J.; Schaefer, H. F., III.; Stephen Binkley, J. J Chem Phys 1986, 85, 6251.
18. Frisch, M. J.; Yamaguchi, Y.; Gaw, J. F.; Schaefer H. F., III; Stephen Binkley, J. J Chem Phys 1986, 84, 531.
19. Atkins, P. W.; Friedman, R. S. Molecular Quantum Mechanics, 3rd Ed.; Oxford University Press: Oxford, 1997, p. 383.
20. Bacskay, G. B.; Saebø, S.; Taylor, P. R. Chem Phys 1984, 90, 215.
21. Komornicki, A.; McIver, J. W. J Chem Phys 1979, 70, 2014.
22. Ioannou, A. G.; Amos, R. D. Chem Phys Lett 1997, 279, 17.
23. Van Caillie, C.; Amos, R. D. Phys Chem Chem Phys 2000, 2, 2123.
24. Kind, C.; Reiher, M.; Neugebauer, J.; Hess, B. A. SNF: A program for quantum chemical calculations of vibrational spectra; University of Erlangen-Nürnberg: 1999–2001.
25. Hess, B. A.; Neugebauer, J.; Reiher, M.; Kind, C. SNFDC: Data collecting program for SNF; University of Erlangen-Nürnberg: 2002. (Based on earlier work by S. Grimme, 1998, University of Bonn, with contributions from M. Gastreich and C. Marian).
26. Ahlrichs, R.; Bär, M.; Häser, M.; Horn, H.; Kölmel, C. Chem Phys Lett 1989, 162, 165.
27. Helgaker, T.; Jensen, H. J. Aa.; Jørgensen, P.; Olsen, J.; Ruud, K.; Ågren, H.; Auer, A. A.; Bak, K. L.; Bakken, V.; Christiansen, O.; Coriani, S.; Dahle, P.; Dalskov, E. K.; Enevoldsen, T.; Fernandez, B.; Hättig, C.; Hald, K.; Halkier, A.; Heiberg, H.; Hettema, H.; Jonsson, D.; Kirpekar, S.; Kobayashi, R.; Koch, H.; Mikkelsen, K. V.; Norman, P.; Packer, M. J.; Pedersen, T. B.; Ruden, T. A.; Sanchez, A.; Saue, T.; Sauer, S. P. A.; Schimmelpfennig, B.; Sylvester-Hvid, K. O.; Taylor, P. R.; Vahtras, O. DALTON, a molecular electronic structure program, Release 1.2; 2001.
28. Schäfer, A.; Huber, C.; Ahlrichs, R. J Chem Phys 1994, 100, 5829.
29. Sadlej, A. J. Theor Chim Acta 1991, 79, 123.
30. Perera, S. A.; Bartlett, R. J. Chem Phys Lett 1999, 314, 381.

31. McDowell, S. A. C.; Amos, R. D.; Handy, N. C. Chem Phys Lett 1995, 235, 1.
32. Kobayashi, R.; Koch, H.; Jørgensen, P. Chem Phys Lett 1994, 219, 30.
33. Halls, M. D.; Schlegel, H. B. J Chem Phys 1999, 111, 8819.
34. Bermejo, D.; Escribano, R.; Orza, J. M. J Mol Spec 1977, 65, 345.
35. Perdew, J. P. Phys Rev B 1986, 33, 8822.
36. Becke, A. D. Phys Rev A 1988, 38, 3098.
37. Bethune, D. S.; Meijer, G.; Tang, W. C.; Rosen, H. J.; Golden, W. G.; Seki, H.; Brown, C. A.; de Vries, M. S. Chem Phys Lett 1991, 179, 181.
38. Albrecht, A. C. J Chem Phys 1961, 34, 1476.
39. Chase, B.; Fagan, P. J. J Am Chem Soc 1992, 114, 2252.
40. van Loosdrecht, P. H. M.; van Bentum, P. J. M.; Verheijen, M. A.; Meijer, G. Chem Phys Lett 1992, 198, 587.
41. Christiansen, O.; Hättig, C.; Jørgensen, P. Spec Act A, 1999, 55, 509.
42. Alms, G. R.; Burham, A. W.; Flygare, W. H. J Chem Phys 1975, 63, 3321.
43. Norman, P.; Luo, Y.; Jonsson, D.; Ågren, H. J Chem Phys 1997, 106, 8788.
44. Meth, J. S.; Vanherzeele, H.; Wang, Y. Chem Phys Lett 1992, 197, 26.